SF2A 2018
P. Di Matteo, F. Billebaud, F. Herpin, N. Lagarde, J.-B. Marquette, A. Robin, O. Venot (eds)

MASS, RADIUS, AND COMPOSITION OF THE TRANSITING PLANET 55 CNC E : USING INTERFEROMETRY AND CORRELATIONS

A. Crida[1, 2], R. Ligi[3], C. Dorn[4] and Y. Lebreton[5, 6]

Abstract. The characterization of exoplanets relies on that of their host star. However, stellar evolution models cannot always be used to derive the mass and radius of individual stars, because many stellar internal parameters are poorly constrained. Here, we use the probability density functions (PDF) of directly measured parameters to derive the joint PDF of the mass and radius of the star 55 Cnc. We find that they are strongly correlated because linked by the stellar density. From this, we derive the joint PDF of the planetary mass and radius of 55 Cnc e.

We then use a planetary interior model to characterize the structure of 55 Cnc e, and to estimate the information content of different sets of data (mass-radius correlation, bulk stellar abundances...). In particular, using updated transit parameters and stellar distance, we constrain the planetary density to within 5% uncertainty, and assess that the radius of the gas layer is 0.03 ± 0.02 planetary radius.

Keywords: stars: fundamental parameters — stars: individual (55 Cnc) — planets and satellites: individual (55 Cnc e) — planets and satellites: composition — methods: analytical

1 Introduction

Planet parameters are never as good as stellar parameters are. It is well known that the transit method provides the ratio between the radius of an exoplanet and that of its host star : $R_p/R_\star = \sqrt{TD}$, where TD holds for the transit depth. Similarly, the radial velocity method gives the mass of an exoplanet M_p as a function of that of its star $M_\star$ and of K, the semi amplitude of the oscillation of the radial velocity of the star. Often, the relative uncertainty on $M_\star$ and $R_\star$ is larger than that on TD and K ; it is nonetheless sometimes not given and/or neglected, which is bad.

How to determine $R_\star$ and $M_\star$ then ? Most often, this is done by fitting stellar evolution models on the observed luminosity and effective temperature of the star. However, this leads to a degeneracy between an old and a young solution (see Bonfanti et al. 2015; Ligi et al. 2016), and these models suffer internal and external sources of errors and depend on many unknown parameters. A more direct solution is to measure the angular diameter of a star by interferometry ; this provides $R_\star$ with up to 2% precision. A good knowledge of the stellar radius then constrains all the other stellar parameters (Creevey et al. 2007). Here, we want to use this tool to narrow the possible radii, masses, and therefore composition of transiting exoplanets. We present a general method, and apply it to the case of 55 Cnc e and its host star 55 Cnc. This work has been published in ApJ just before the conference (Crida et al. 2018a), and updated shortly after (Crida et al. 2018b).

[1] Université Côte d'Azur / Observatoire de la Côte d'Azur — Lagrange (UMR 7293), Boulevard de l'Observatoire, CS 34229, 06300 Nice, France

[2] Institut Universitaire de France, 103 Boulevard Saint-Michel, 75005 Paris, France

[3] INAF-Osservatorio Astronomico di Brera, Via E. Bianchi 46, I-23807 Merate, Italy

[4] University of Zurich, Institut of Computational Sciences, University of Zurich, Winterthurerstrasse 190, CH-8057, Zurich, Switzerland

[5] LESIA, Observatoire de Paris, PSL Research University, CNRS, Université Pierre et Marie Curie, Université Paris Diderot, 92195 Meudon, France

[6] Institut de Physique de Rennes, Universit de Rennes 1, CNRS UMR 6251, 35042 Rennes, France

2 A (not so useful) Bayesian approach

The observations at hand for the star are θ the angular diameter, $p_\star$ the parallax, and m the magnitude from which one deduces $F_{\rm bol}$ the bolometric flux. Using the well-known relations $L = 4F_{\rm bol}\,(1\ {\rm pc}/p_\star)^2$ and $T_{\rm eff} = (4F_{\rm bol}/\sigma_{\rm SB}\theta)^{1/4}$ (with $\sigma_{\rm SB}$ the Stefan-Boltzmann constant), one can express the joint likelihood of the luminosity L and temperature $T_{\rm eff}$ of the star as a function of the probability density functions (PDFs) of the observed quantities (here, θ is given in milliarceseconds (mas) and m_r is the number of mas in one radian) :

$$\mathcal{L}_{\rm HR}(L,T_{\rm eff}) = \frac{4\,{\rm pc}\,\sqrt{\pi}m_r}{T_{\rm eff}^3\sqrt{\sigma_{\rm SB}L^3}} \times \int_0^{+\infty} t \times f_{F_{\rm bol}}(t) \times f_{p_\star}\left(\sqrt{\frac{4\pi t}{L}}\right) \times f_\theta\left(\sqrt{\frac{4\,t}{\sigma_{\rm SB}\,T_{\rm eff}^4}}\right)\,{\rm d}t\ . \tag{2.1}$$

But the density of stars in the H-R diagram is *a priori* known. We have computed the density of stars around 55 Cnc from the *Hipparcos* catalog, $f^0_{\rm Hip}(L,T_{\rm eff})$, which we can use as a prior to derive the joint PDF of $M_\star - R_\star$ for 55 Cnc as :

$$f_{\rm HR}(L,T_{\rm eff}) = \mathcal{L}_{\rm HR}(L,T_{\rm eff}) \times f^0_{\rm Hip}(L,T_{\rm eff})\ .$$

The result is not significantly changed. Interferometry allows to constrain L and $T_{\rm eff}$ so precisely that the use of the prior is not helpful. Therefore, in what follows, we take $f_{\rm HR} = \mathcal{L}_{\rm HR}$ as given by Eq. (2.1).

3 Direct probability density function : the star

In the case of a planet on a circular orbit exactly in the line of sight, the duration of the transit $T = 2R_\star/a\Omega$ and its period $P = 2\pi/\Omega$ (where a is the orbital radius and Ω the orbital angular velocity) combine to give the stellar density : $P/T^3 = (\pi^2 G/3)\rho_\star$ (Seager & Mallén-Ornelas 2003). In the case of 55 Cnc, $\rho_\star$ is given by Maxted et al. (2015), so that measuring $R_\star$ provides a direct estimate of $M_\star$ without the use of any stellar model. More precisely, we provide the joint PDF of $M_\star - R_\star$:

$$\mathcal{L}_{MR\star}(M,R) = \frac{3}{4\pi R^3} \times f_{R_\star}(R) \times f_{\rho_\star}\left(\frac{3M}{4\pi R^3}\right) \tag{3.1}$$

The left panel of Figure 1 shows this PDF in the case of 55 Cnc as plain black contours. The correlation is very strong (0.85). If one neglects the correlation and takes the values of $M_\star$ and $R_\star$ with their uncertainties considered independently, one gets PDF represented by the blue dashed contours. It has the same marginal distributions, but it is not correct, and allows for unrealistic stellar densities.

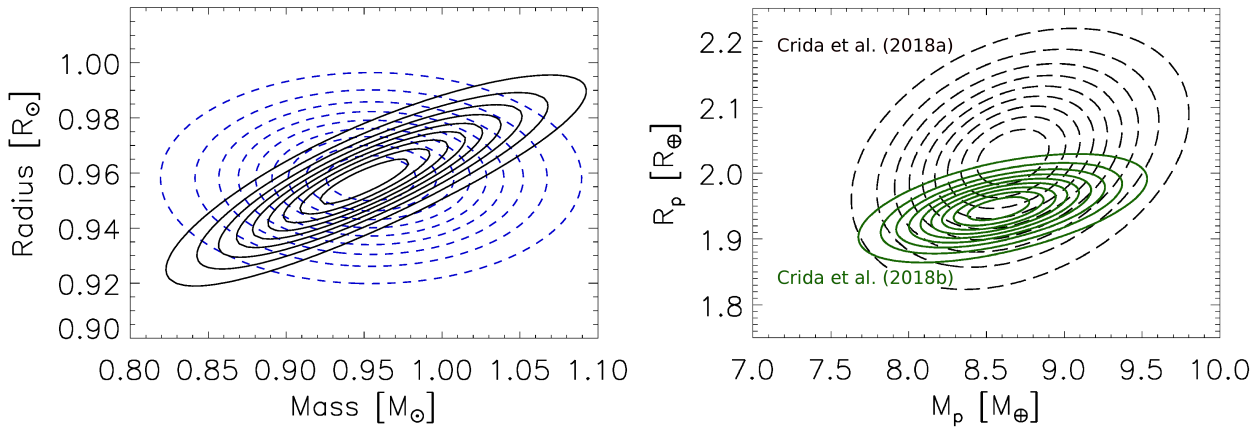

Fig. 1. Left : Joint probability density function of the mass and radius of the star 55 Cnc. The 9 plain thick contour lines separate 10 equal-sized intervals between 0 and the maximum of Eq. (3.1). The dashed blue contour lines show the same for the case where one mistakenly considers $M_\star$ and $R_\star$ as independent. **Right :** Same, for the planet 55 Cnc e. Black, long dashed contours : PDF obtained in the original paper Crida et al. (2018a), based on the black PDF for the star in the left panel. Dark green, plain contours : PDF obtained in the update (Crida et al. 2018b) using new, more precise data for TD, K and $p_\star$.

4 Direct probability density function : the planet

For any M_p, $M_\star$, one can define the associated semi amplitude of the radial velocity signal K, following a classical formula resulting from Kepler's law: $K(M_p, M_\star) = \frac{M_p}{M_\star^{2/3}} \left(\frac{2\pi G}{P}\right)^{1/3}$ (where P is the orbital period, and we have assumed that the eccentricity is zero*). Similarly, for a pair R_p, $R_\star$, the corresponding transit depth is $TD(R_p, R_\star) = (R_p/R_\star)^2$. Therefore, the probability density function associated to any fixed planetary mass and radius is :

$$f_p(M_p, R_p) \propto \iint \exp\left(-\frac{\left(K(M_p, M_\star) - K_e\right)^2}{2\,{\sigma_K}^2}\right) \exp\left(-\frac{\left(TD(M_p, M_\star) - TD_e\right)^2}{2\,{\sigma_{TD}}^2}\right) \mathcal{L}_{MR\star}(M_\star, R_\star)\ \mathrm{d}M_\star\,\mathrm{d}R_\star\ . \tag{4.1}$$

With $TD_e \pm \sigma_{TD} = (3.72 \pm 0.30)10^{-4}$ the transit depth associated to 55 Cnc e (Dragomir et al. 2014), and $K_e \pm \sigma_K = 6.30 \pm 0.21$ m/s the amplitude of the signal in radial velocity (Endl et al. 2012), this gives (Crida et al. 2018a) :

$$R_p = 2.023 \pm 0.088\ R_\oplus \quad ; \quad M_p = 8.703 \pm 0.482\ M_\oplus \tag{4.2}$$

with a correlation of $c = 0.30$. It is shown as the black dashed contours in the right panel of figure 1. The correlation is not as strong as in the stellar case (black solid contours, left panel) because of the rather large uncertainty on TD.

Shortly after the SF2A week, Bourrier et al. (2018) published new data for 55 Cnc e, in particular exquisitely precise transit parameters. In addition, 55 Cnc is in the Gaia DR2, with a parallax more precise but inconsistent with the one we used. This allowed us to correct and refine our estimates of the stellar and planetary parameters. The new contours for the joint PDF of $M_p - R_p$ are the solid green ones in the right panel of figure 1, and we finally have (Crida et al. 2018b) :

$$R_p = 1.947 \pm 0.038\,R_\oplus \quad ; \quad M_p = 8.59 \pm 0.43\,M_\oplus\ , \tag{4.3}$$

with a correlation $c = 0.54$ and

$$\rho_p = 1.164 \pm 0.062\,\rho_\oplus = 6421 \pm 342\ \mathrm{kg.m^{-3}}\ . \tag{4.4}$$

The reader is advised to use these numbers instead of the ones in Eq. (4.2).

5 Planetary interior parameters

The planetary mass and radius can now be fed into a planetary interior model. We use the model developed by Dorn et al. (2017) that employs an MCMC method to determine the size of the core, the elemental ratios of Fe/Si and Mg/Si in the mantle, the size of the rocky interior, and the properties of the gas layer. We assume that the planet has no water layer, and that its chemistry dominated by O not C. The data we use can be decomposed into the Original data (`O` : planetary mass and radius without correlation, orbital radius and stellar irradiation), the correlation between mass and radius (`C`), and the stellar abundances (`A`) that comprise the bulk element ratios Fe/Si, Mg/Si, and minor elements. We add a hypothetical data `H`, that would correspond to zero uncertainty in TD and K, to see how this would help constraining the internal parameters.

In Crida et al. (2018a), we used the planetary mass and radius given by Eq. (4.2) and studied the significance of the data sets. We considered different scenarios, labeled `O`, `OC`, `OA`, `OH` and `OCA` after the data taken into account. The cumulative distribution function of all the parameters is shown in figure 2 for all the scenarios. It shows that `A` helps mainly for the composition of the mantle, while `C` refines our estimate of the gas layer and `H` would allow to rule out a purely solid composition.

Adding up all the data, the `OCA` scenario is the best to constrain all the parameters of 55 Cnc e. Therefore, in Crida et al. (2018b), we apply this scenario to the data given by Eq. (4.3), and we eventually find that the radius of the gas layer is $0.03 \pm 0.02\,R_p$.

*The eccentricity of 55 Cnc e is 0.028 in `exoplanet.eu`, which makes the assumption $e \approx 0$ reasonable.

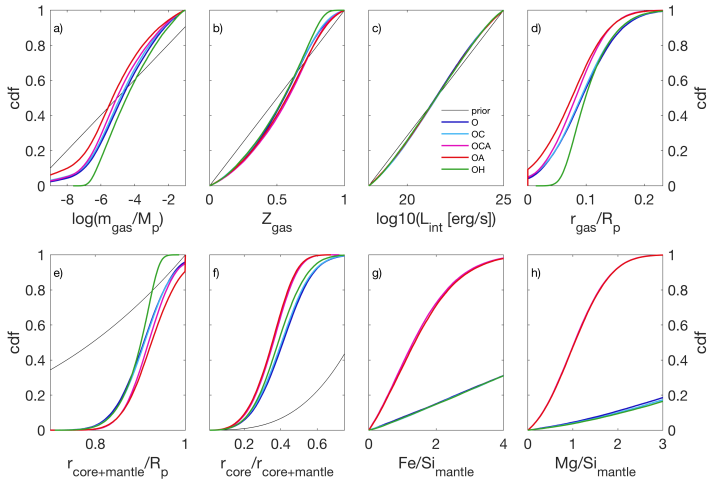

Fig. 2. Sampled one-dimensional marginal posterior for interior parameters: (a) gas mass fraction $m_{\rm gas}$, (b) gas metallicity $Z_{\rm gas}$, (c) intrinsic luminosity $L_{\rm int}$, (d) gas radius fraction, (e) size of rocky interior $r_{\rm core+mantle}/{\rm R_p}$, (f) relative core size $r_{\rm core}/r_{\rm core+mantle}$, (g, h) mantle composition in terms of mass ratios ${\rm Fe/Si_{mantle}}$ and ${\rm Mg/Si_{mantle}}$. The prior distributions are shown in black. For (g, h) the priors vary between the data scenarios (`O`, `OC`, `OH` versus `OCA`, `OA`) and are not shown. **Warning:** here, we used obsolete planetary mass and radius, so that these curves are not relevant for themselves, but for how they differ depending on the data taken into account.

6 Conclusions

Using interferometry to measure the angular diameter of a star hosting a transiting exoplanet offers many advantages. Because the transit light-curve provides an estimate of the stellar density, the stellar mass can be found without the use of any model. And the stellar mass and radius show a strong correlation, such that the planetary density which derives from the stellar parameters is also better constrained. This in turn allows for a more precise estimate of all the planetary interior parameter. Neglecting the correlation would lead to larger uncertainties, and inaccurate estimates. Therefore, this method should be generalized and applied whenever possible. The stars target of the future transit space missions will be brighter than the Kepler targets, hopefully allowing interferometry to come often into play.

In the case of 55 Cnc e, recent data allowed us to give the planetary density with only 5% relative uncertainty, and thus to quantify the thickness of the gas layer, among many other planetary parameters.

We thank the organizers of the SF2A conference in Bordeaux.
A.C. is supporter of the French football team, who performed great at the world cup before, during, and after the conference.

References

Bonfanti, A., Ortolani, S., Piotto, G., & Nascimbeni, V. 2015, A&A, 575, A18

Bourrier, V., Dumusque, X., Dorn, C., et al. 2018, ArXiv e-prints

Creevey, O. L., Monteiro, M. J. P. F. G., Metcalfe, T. S., et al. 2007, ApJ, 659, 616

Crida, A., Ligi, R., Dorn, C., & Lebreton, Y. 2018a, ApJ, 860, 122

Crida, A., Ligi, R., Dorn, C., Borsa, F., & Lebreton, Y. 2018b, RNAAS, 2, 172

Dorn, C., Venturini, J., Khan, A., et al. 2017, A&A, 597, A37

Dragomir, D., Matthews, J. M., Winn, J. N., & Rowe, J. F. 2014, in IAU Symposium, Vol. 293, Formation, Detection, and Characterization of Extrasolar Habitable Planets, ed. N. Haghighipour, 52–57

Endl, M., Robertson, P., Cochran, W. D., et al. 2012, ApJ, 759, 19

Ligi, R., Creevey, O., Mourard, D., et al. 2016, A&A, 586, A94

Maxted, P. F. L., Serenelli, A. M., & Southworth, J. 2015, A&A, 575, A36

Seager, S. & Mallén-Ornelas, G. 2003, ApJ, 585, 1038